Very-High-Energy Gamma Rays from a Distant Quasar: How Transparent Is the Universe?

The MAGIC Collaboration*

Science **320**, 1752 (2008); DOI: 10.1126/science.1157087

Keywords: 3C 279, Quasar, EBL, Cherenkov telescope

The atmospheric Cherenkov gamma-ray telescope MAGIC, designed for a low-energy threshold, has detected very-high-energy gamma rays from a giant flare of the distant Quasi-Stellar Radio Source (in short: radio quasar) 3C 279, at a distance of more than 5 billion light-years (a redshift of 0.536). No quasar has been observed previously in very-high-energy gamma radiation, and this is also the most distant object detected emitting gamma rays above 50 gigaelectron volts. Since high-energy gamma rays may be stopped by interacting with the diffuse background light in the universe, the observations by MAGIC imply a low amount for such light, consistent with that known from galaxy counts.

Ground-based gamma-ray telescopes are sensitive to the Cherenkov light emitted by the electromagnetic showers that are produced by gamma rays interacting in the atmosphere. These telescopes have discovered, since the first detection (in 1989) of gamma rays in this energy range (from 100 GeV to several TeV), more than 20 blazars, which are thought to be powered by accretion of matter onto supermassive black holes residing in the centers of galaxies, and ejecting relativistic jets at small angles to the line of sight (*1*). Most of these objects are of the BL Lac type, with weak or no optical emission lines. Quasar 3C 279 shows optical emission lines that allow a good redshift determination. Satellite observations with the Energetic Gamma Ray Experiment Telescope (EGRET) aboard the Compton Gamma Ray Observatory (CGRO) had measured gamma rays from 3C 279 (*2*) and other quasars, but only up to the energies of a few GeV, the limit of the detector's sensitivity. An upper limit for the flux of very-high-energy (VHE) gamma rays was quoted in (*3*).

Using MAGIC, the world's largest single-dish gamma-ray telescope (*4*) on the Canary island of La Palma (2200 m above sea level, 28.4°N, 17.54°W), we detected gamma rays at energies from 80 to >300 GeV, emanating from 3C 279 at a redshift of 0.536, which corresponds to a light-travel time of 5.3 billion years. No object has been seen before in this range of VHE gamma-ray energies at such a distance [the highest redshift previously observed was 0.212 (*5*)], and no quasar has been previously identified in this range of gamma-ray energies.

*The complete list of authors and their affiliations appears at the end of this paper.

The detection of 3C 279 is important, because gamma rays at very high energies from distant sources are expected to be strongly attenuated in intergalactic space by the possible interaction with low-energy photons ($\gamma + \gamma \rightarrow e^+ + e^-$). These photons [extragalactic background light (EBL) (*6*)] have been radiated by stars and galaxies in the course of cosmic history. Their collective spectrum has evolved over time and is a function of distance. For 3C 279, the range of newly probed EBL wavelengths lies between 0.2 and 0.8 μm (ultraviolet/optical). Existing instruments that are sensitive only to higher gamma-ray energies have so far been unable to probe this domain; by contrast, MAGIC is specifically designed to reach the lowest-energy threshold among ground-based detectors.

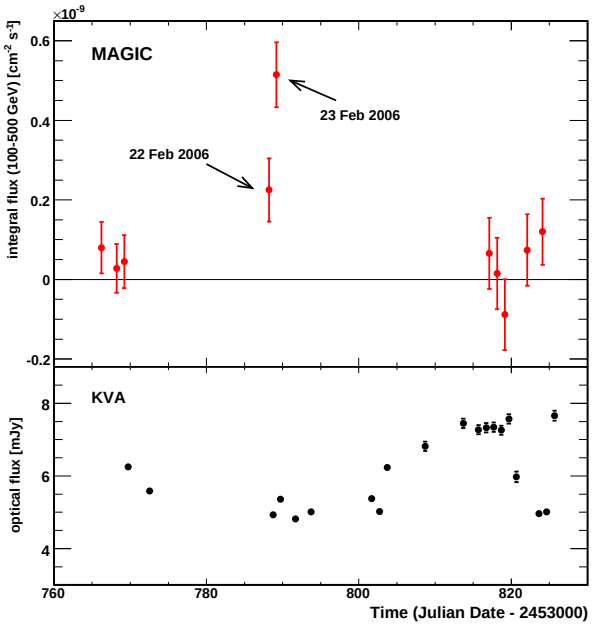

Fig. 1. Light curves. MAGIC (top) and optical R-band data (bottom) obtained for 3C 279 from February to March 2006. The long-term baseline for the optical flux is at 3 mJy.

In observations of 3C 279 over ten nights between late January and April 2006 (total of 9.7 hours), the gamma-ray source was clearly detected (at >6 SDs) on the night of 23 February, and may also have been detected the night before (Fig. 1). As determined by the χ^2 test, the probability that the gamma-ray flux on all 10 nights was zero is 2.3×10^{-7}, corresponding to

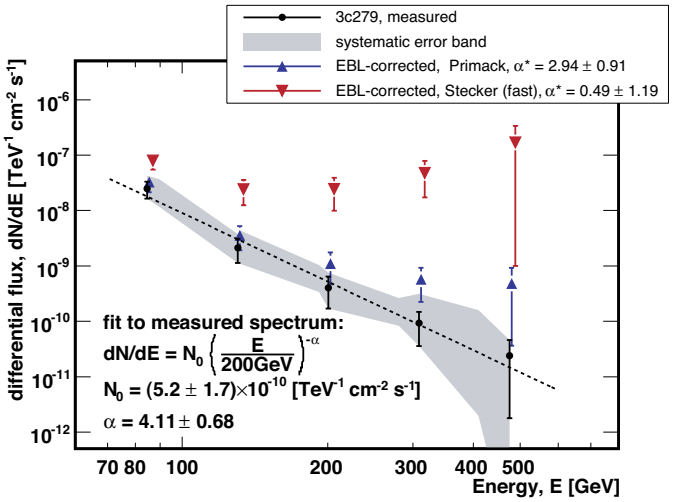

Fig. 2. Spectrum of 3C 279 measured by MAGIC. The grey area includes the combined statistical (1σ) and systematic errors, and underlines the marginal significance of detections at high energy. The dotted line shows compatibility of the measured spectrum with a power law of photon index $\alpha = 4.1$. The blue and red triangles are measurements corrected on the basis of the two models for the EBL density, discussed in the text.

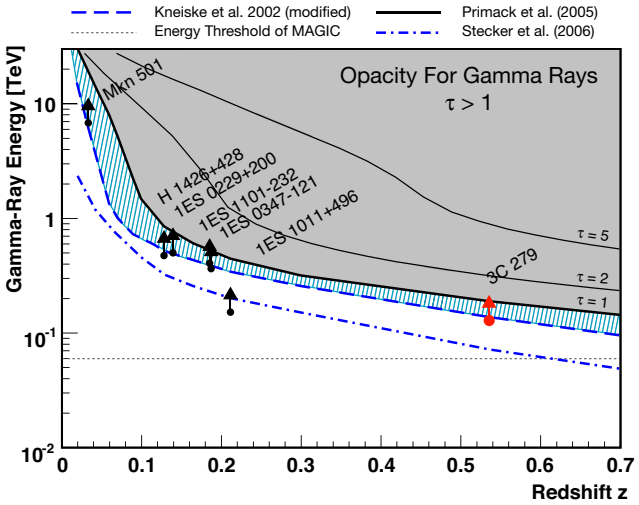

Fig. 3. The gamma-ray horizon. The redshift region over which the gamma-ray horizon can be constrained by observations has been extended up to z=0.536. The prediction range of EBL models is illustrated by (*8*) (thick solid black line) and (*11*) (dashed-dotted blue line). The tuned model of (*14*) (dashed blue line) represents an upper EBL limit based on our 3C 279 data, obtained on the assumption that the intrinsic photon index is ≥ 1.5 (red arrow). Limits obtained for other sources are shown by black arrows, most of which lie very close to the model (*14*). The narrow blue band is the region allowed between this model and a maximum possible transparency (i.e., minimum EBL level) given by (*8*), which is nearly coincident with galaxy counts. The gray area indicates an optical $\tau > 1$, i.e., the flux of gamma rays is strongly suppressed. To illustrate the strength of the attenuation in this area, we also show energies for $\tau = 2$ and $\tau = 5$ (thin black lines), again with (*8*) as model.

5.04σ in a Gaussian distribution [see (*7*)]. Simultaneous optical R-band observations, by the Tuorla Observatory Blazar Monitoring Program with the 1.03 m telescope at the Tuorla Observatory, Finland, and the 35 cm Kungliga Vetenskapsakademien (Royal Swedish Academy of Sciences) telescope on La Palma, revealed that during the MAGIC observations, the gamma-ray source was in a generally high optical state, a factor of 2 above the long-term baseline flux, but with no indication of short time-scale variability at visible wavelengths. The observed VHE spectrum (Fig. 2) can be described by a power law with a differential photon spectral index of $\alpha = 4.1 \pm 0.7_{\rm stat} \pm 0.2_{\rm syst}$. The measured integrated flux above 100 GeV on 23 February is $(5.15 \pm 0.82_{\rm stat} \pm 1.5_{\rm syst}) \times 10^{-10}$ photons cm^{-2} s^{-1}.

The EBL influences the observed spectrum and flux, resulting in an exponential decrease with energy and a cutoff in the gamma-ray spectrum. Several models have been proposed for the EBL (*6*). All have limited predictive power for the EBL density, particularly as a function of time, because many details of star and galaxy evolution remain uncertain. We illustrate the uncertainty in the EBL by using two extreme models: a model by Primack *et al.* (*8*), close to the lowest possible attenuation level consistent with lower EBL limit from galaxy counts (*9, 10*); and a "fast-evolution" model by Stecker *et al.* (*11*), corresponding to the highest attenuation of all the models. We refer to these models as "low" and "high," respectively. The measured spectra of 3C 279, corrected for absorption according to these two models, are shown in Fig. 2. They represent the range for the possible intrinsic gamma-ray flux of the source.

A power-law fit to the EBL-corrected points (*12*) results in an intrinsic photon index of $\alpha^* = 2.9 \pm 0.9_{\rm stat} \pm 0.5_{\rm syst}$ (low) and $\alpha^* = 0.5 \pm 1.2_{\rm stat} \pm 0.5_{\rm syst}$ (high). The systematic error is determined by shifting the absolute energy scale by the estimated energy error of 20% and recalculating the intrinsic spectrum. Further discussion of the intrinsic spectrum and the spectral energy density can be found in (*7*).

The measured spectrum of 3C 279 permits a test of the transparency of the universe to gamma rays. The distance at which the flux of photons of a given energy is attenuated by a factor e (i.e., the path corresponding to an optical depth $\tau = 1$) is called the gamma-ray horizon and is commonly expressed as a function of the redshift parameter (*13*); we show this energy/redshift relation in Fig. 3. In the context of Fig. 3, we make use of a model based on (*14*) with parameters adapted to the limits given by (*15*) and fine-tuned such that for 3C 279, the intrinsic photon index is $\alpha^* = 1.5$. The tuning allows for the statistical and systematic errors (1 SD, added linearly). Although the intrinsic spectrum emitted by 3C 279 is unknown, $\alpha^* = 1.5$ is the lowest value given for EGRET sources (not affected by the EBL) and all spectra measured by gamma-ray telescopes so far (*16*), so we assume this to be the hardest acceptable spectrum. The region allowed between the maximum EBL determined using the above procedure and that from galaxy counts (*8*) is very small.

The results support, at higher redshift, the conclusion drawn from earlier measurements (*15*) that the observations of the

Hubble Space Telescope and Spitzer correctly estimate most of the light sources in the universe. The derived limits are consistent with the EBL evolution corresponding to a maximum star-formation rate at $z \geq 1$, as suggested by (*8*) and similar models.

The emission mechanism responsible for the observed VHE radiation remains uncertain. Leptonic emission models (assuming relativistic electrons in the jet as source of the gamma rays), generally successful in describing blazar data [e.g., (*17*)], can, with some assumptions, also accommodate the MAGIC spectrum. Hadronic models [involving relativistic protons, e.g. (*18*)] provide a possible alternative. However, a genuine test of the models can be only obtained with simultaneous observations at different wavelengths, which are not available for the observations described here. Future tests of these models should use observations from sources at all wavelengths from radio to VHE gamma rays. In the domain of VHE gamma rays, we can expect important new insights by simultaneous observations with the Large Area Telescope (LAT), the high-energy gamma-ray instrument on the Gamma Ray Large Area Space Telescope [GLAST (*19*)]. Our observations of this distant source in VHE gamma rays demonstrate that a large fraction of the universe is accessible to VHE astronomy.

References

1. R. D. Blandford, M. J. Rees, *Astrophys. Lett.* **10**, 77 (1972).
2. R. C. Hartman *et al.*, *Astrophys. J.* **385**, L1 (1992).
3. F. Aharonian *et al.*, *Astron. Astrophys.* **478**, 387 (2008).
4. E. Lorenz, *New Astronomy Review* **48**,339 (2004).
5. J. Albert *et al.*, *Astrophys. J.* **667**, L21 (2007).
6. M. G. Hauser, E. Dwek, *Ann. Rev. Astron. Astrophys.* **39**, 307 (2001).
7. Further information on data and methods and additional discussion are available on *Science Online*.
8. J. R. Primack, J. S. Bullock, R. S. Somerville, in *High Energy Gamma-Ray Astronomy*, American Institute of Physics Conference Series, F. Aharonian, H. Voelk, D. Horns, Eds. (American Institute of Physics, Heidelberg, 2005), vol. 745, p. 23.
9. P. Madau, L. Pozzetti, *Mon. Not. R. Astron. Soc.* **312**, L9 (2000).
10. G. Fazio *et al.*, *Astrophys. J. Suppl. Ser.* **154**, 39 (2004).
11. F. W. Stecker, M. A. Malkan, S. T. Scully, *Astrophys. J.* **648**, 774 (2006).
12. We approximate the intrinsic energy spectrum by $dN/dE \propto E^{-\alpha^*}$, where α^* is the intrinsic photon spectral index.
13. G. G. Fazio, F. W. Stecker, *Nature* **226**, 135 (1970).
14. T. M. Kneiske, K. Mannheim, D. H. Hartmann, *Astron. Astrophys.* **386**, 1 (2002).
15. F. Aharonian *et al.*, *Nature* **440**, 1018 (2006).
16. According to recent simulations (*20*), photon indices of $<.5$ can not be entirely excluded.
17. L. Maraschi, G. Ghisellini, A. Celotti, *Astrophys. J.* **397**, L5 (1992).
18. K. Mannheim, P. L. Biermann, *Astron. Astrophys.* **251**, L21 (1992).
19. S. Funk *et al.*, (GLAST-LAT Collaboration), *GLAST and ground-based gamma ray astronomy*, SLAC-PUB-12871; www-glast.stanford.edu/.
20. F. W. Stecker, M. G. Baring, E. J. Summerlin, *Astrophys. J.* **667**, L29 (2007).

21. We thank the Instituto de Astrofisica de Canarias for the excellent working conditions at the Observatorio del Roque de los Muchachos in La Palma, Canary Islands. The support of the German Bundesministerium für Bildung und Forschung and Max-Planck Gesellschaft, the Italian Istituto Nazionale di Fisica Nucleare (INFN) and Spanish Centro de Investigaciòn Cientifica y Technologia is gratefully acknowledged. This work was also supported by ETH (research grant TH 34/043) and the Polish MNil (grant 1P03D01028).

The MAGIC Collaboration: J. Albert,[1] E. Aliu,[2] H. Anderhub,[3] L. A. Antonelli,[4] P. Antoranz,[5] M. Backes,[6] C. Baixeras,[7] J. A. Barrio,[5] H. Bartko,[8] D. Bastieri,[9] J. K. Becker,[6] W. Bednarek,[10] K. Berger,[1] E. Bernardini,[11] C. Bigongiari,[9] A. Biland,[3] R. K. Bock,[8,9*] G. Bonnoli,[12] P. Bordas,[13] V. Bosch-Ramon,[13] T. Bretz,[1] I. Britvitch,[3] M. Camara,[5] E. Carmona,[8] A. Chilingarian,[14] S. Commichau,[3] J. L. Contreras,[5] J. Cortina,[2] M. T. Costado,[15,16] S. Covino,[4] V. Curtef,[6] F. Dazzi,[9] A. De Angelis,[17] E. De Cea del Pozo,[18] R. de los Reyes,[5] B. De Lotto,[17] M. De Maria,[17] F. De Sabata,[17] C. Delgado Mendez,[15] A. Dominguez,[19] D. Dorner,[1] M. Doro,[9] M. Errando,[2] M. Fagiolini,[12] D. Ferenc,[20] E. Fernández,[2] R. Firpo,[2] M. V. Fonseca,[5] L. Font,[7] N. Galante,[8] R. J. García López,[15,16] M. Garczarczyk,[8] M. Gaug,[15] F. Goebel,[8] M. Hayashida,[8] A. Herrero,[15,16] D. Höhne,[1] J. Hose,[8] C. C. Hsu,[8] S. Huber,[1] T. Jogler,[8] T. M. Kneiske,[6] D. Kranich,[3] A. La Barbera,[4] A. Laille,[20] E. Leonardo,[12] E. Lindfors,[12] S. Lombardi,[9] F. Longo,[17] M. López,[9] E. Lorenz,[3,8] P. Majumdar,[8] G. Maneva,[22] N. Mankuzhiyil,[17] K. Mannheim,[1] L. Maraschi,[4] M. Mariotti,[9] M. Martínez,[2] D. Mazin,[2] M. Meucci,[12] M. Meyer,[1] J. M. Miranda,[5] R. Mirzoyan,[8] S. Mizobuchi,[8] M. Moles,[19] A. Moralejo,[2] D. Nieto,[5] K. Nilsson,[21] J. Ninkovic,[8] N. Otte,[8,23†] I. Oya,[5] M. Panniello,[15‡] R. Paoletti,[12] J. M. Paredes,[13] M. Pasanen,[21] D. Pascoli,[9] F. Pauss,[3] R. G. Pegna,[12] M. A. Perez-Torres,[19] M. Persic,[17,24] L. Peruzzo,[9] A. Piccioli,[12] F. Prada,[19] E. Prandini,[9] N. Puchades,[2] A. Raymers,[14] W. Rhode,[6] M. Ribó,[13] J. Rico,[25,2] M. Rissi,[3] A. Robert,[7] S. Rügamer,[1] A. Saggion,[9] T. Y. Saito,[8] M. Salvati,[4] M. Sanchez-Conde,[19] P. Sartori,[9] K. Satalecka,[11] V. Scalzotto,[9] V. Scapin,[17] R. Schmitt,[1] T. Schweizer,[8] M. Shayduk,[23,8] K. Shinozaki,[8] S. N. Shore,[26] N. Sidro,[2] A. Sierpowska-Bartosik,[18] A. Sillanpää,[21] D. Sobczynska,[10] F. Spanier,[1] A. Stamerra,[12] L. S. Stark,[3] L. Takalo,[21] F. Tavecchio,[4] P. Temnikov,[22] D. Tescaro,[2] M. Teshima,[8] M. Tluczykont,[11] D. F. Torres,[25,18] N. Turini,[12] H. Vankov,[22] A. Venturini,[9] V. Vitale,[17] R. M. Wagner,[8] W. Wittek,[8] V. Zabalza,[13] F. Zandanel,[19] R. Zanin,[2] J. Zapatero[7]

[1] Universität Würzburg, D-97074 Würzburg, Germany. [2] Institut de Física d'Altes Energies, Edifici Cn., Campus UAB, E-08193 Bellaterra, Spain. [3] ETH Zurich, CH-8093 Switzerland. [4] Istituto Nazionale di Astrofisica (INAF) National Institute for Astrophysics, I-00136 Rome, Italy. [5] Universidad Complutense, E-28040 Madrid, Spain. [6] Technische Universität Dortmund, D-44221 Dortmund, Germany. [7] Universitat Autònoma de Barcelona, E-08193 Bellaterra, Spain. [8] Max-Planck-Institut für Physik, D-80805 München,

Germany. [9] Università di Padova and INFN, I-35131 Padova, Italy. [10] University of Łódź, PL-90236 Łódź, Poland. [11] DESY Deutsches Elektronen-Synchrotron, D-15738 Zeuthen, Germany. [12] Università di Siena, and INFN Pisa, I-53100 Siena, Italy. [13] Universitat de Barcelona Insitut de Ciencias del Cosmos–Institut d'Estudis Especials de Catalunya (IEEC), E-08028 Barcelona, Spain. [14] Yerevan Physics Institute, AM-375036 Yerevan, Armenia. [15] Instituto de Astrofisica de Canarias, E-38200, La Laguna, Tenerife, Spain. [16] Departamento de Astrofisica, Universidad, E-38206 La Laguna, Tenerife, Spain. [17] Università di Udine, and INFN Trieste, I-33100 Udine, Italy. [18] Institut de Cienciès de l'Espai [IEEC-Consejo Superior de Investigaciones Cíentificas (CSIC)], E-08193 Bellaterra, Spain. [19] Inst. de Astrofisica de Andalucia (CSIC), E-18080 Granada, Spain. [20] University of California, Davis, CA-95616-8677, USA. [21] Tuorla Observatory, Turku University, FI-21500 Piikkiö, Finland. [22] Institute for Nuclear Research and Nuclear Energy, BG-1784 Sofia, Bulgaria. [23] Humboldt-Universität zu Berlin, D-12489 Berlin, Germany. [24] INAF/Osservatorio Astronomico and INFN, I-34143 Trieste, Italy. [25] Institucío Catalana de Recerca i Estudis Avancats, E-08010 Barcelona, Spain. [26] Università di Pisa, and INFN Pisa, I-56126 Pisa, Italy.

*To whom correspondence should be addressed.
E-Mail: rkbock@gmail.com
† Present address: Santa Cruz Institute for Particle Physics, University of California, Santa Cruz, CA 95064, USA.
‡ deceased.

27 February 2008; accepted 27 May 2008
10.1126/science.1157087

Supporting Online Material

www.sciencemag.org/cgi/content/full/320/5884/1752/DC1
SOM Text
Figs. S1 to S3
References

Comments to the Introduction

Ground-based gamma ray astronomy, pioneered by the Whipple Collaboration, has led to a number of important discoveries in recent years, showing an unexpected wealth of sources in the very high-energy (VHE) sky above 100 GeV. Among them, some twenty extragalactic sources were found, all but one are blazars. Blazars are now known in a broad range of luminosities, from low-luminosity BL-Lac objects to high-luminosity quasars. They emit non-thermal radiation from radio waves to gamma rays, originating presumably in synchrotron emission and inverse-Compton scattering. Most blazars so far detected with ground-based telescopes belong to the rare subspecies of BL-Lac objects, that can be interpreted as a kind of dying quasar running out of fuel, and thinning out at large cosmological distances (*1*). 3C 279 is the first blazar of the quasar type observed to emit gamma rays in the VHE range. It had been discovered as a source of lower energy gammas by the EGRET detector (*2*), with a peak flux higher than any other source seen by EGRET. Subsequently 3C 279 became a much-studied source with multi-wavelength observation campaigns published (*3,4,5,6,7,8*).

MAGIC analysis

The observations were carried out in the "on/off mode", which includes "on" events taken with the telescope pointing at the source, and a similar amount of "off" events taken off-axis at a sky location near the source, with very similar operating conditions. The "off" events are necessary for estimating reliably the background of hadronic events.

The raw data were calibrated (*9*) and analyzed with the standard MAGIC analysis and reconstruction software (*10*). Data runs with anomalous trigger rates due to bad observation conditions were rejected. The remaining "on" data correspond to 9.7 hours, with 4.9 hours of "off" data. The standard analysis reduces the image to a single cluster of pixels by removing image noise and tracks far from the main shower, and calculates image parameters from the cleaned image (*11*). These are used by a multi-variate method to discriminate gamma rays from background hadrons; the method is called "Random Forest" (*12*) and is a multi-tree classifier algorithm which calculates, from a combination of image parameters, a separation variable called hadronness.

All image parameters were checked for consistency between "on" and "off" data. The excess events were obtained by subtracting suitably normalized "off" data from the "on" data, as shown in Fig. S1. The variable Alpha is one of the image parameters. It describes the direction of the main alignment axis of the pixels in the image, a zero value indicating a shower seemingly coming (in the camera plane) from the known position of the source. Alpha was not included in the multivariate gamma-hadron separation. Cuts in hadronness and Alpha were optimized using data samples from observations of the Crab Nebula at comparable zenith angles. For the detection (and the lightcurve) we require hadronness<0.12 and Alpha<12°, resulting in an efficiency of 40% for gammas. For these cuts and with a minimal Size of 100 (Size is the sum of signals, in photo-electrons), we obtain a peak in the distribution of estimated energy at 170 GeV.

The significance of the signal of 23 February was calculated according to equation 17 in (*13*), resulting in 6.15σ, taking the difference between a smoothing parabola fit to normalized "off" data and the "on" data. The probability that we deal with a statistical fluctuation in ten independent observations (trial factor corresponding to 10 nights of observation) is 3.87×10^{-9}, which corresponds to a significance of 5.77σ. If "off" and "on" data are compared bin by bin without smoothing, the significance is 5.5σ for 23 February, and 5.1σ after correcting for trials. We also applied a χ^2 test to the results of ten nights, giving 50.35 for 10 degrees of freedom, or a probability of $2.3x10^{-7}$, which in a Gaussian distribution corresponds to 5.04σ. The long-term detector stability has been studied by monitoring the Crab Nebula over a large range of zenith angles, and for several years. The observed integrated flux above 100 GeV has shown no evidence of any variations beyond what is expected from statistics. We can thus conclude that the observed signal is indeed an isolated flare from 3C 279.

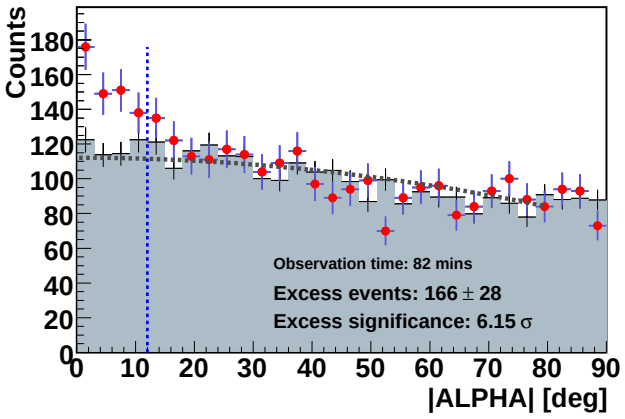

Fig. S1. Histogram of the image parameter Alpha. The image parameter Alpha obtained for 3C 279 in the night of 23 February 2006, for "on" (red dots) and "off" (crosses and filled area) pointings, respectively. The dotted line is a simple parabolic fit (without linear term) to the "off" events between 0° and 80°, serving to smoothen the background for better extrapolation towards Alpha=0; the excess events are obtained with respect to this line.

The reconstruction of gamma ray energy uses an approximation derived from image parameters. It is obtained by the the Random Forest method using Monte Carlo gamma samples. For the reconstruction of the energy spectrum, we used a low-energy analysis, making also use of the timing properties of the air showers with a lower energy threshold (≈110 GeV). The cuts for obtaining the spectrum were slightly loosened, resulting in a gamma efficiency of 50%. The obtained spectrum

was unfolded for detector effects using (*14*). The spectrum was cross-checked with two alternative methods (one of them is the standard analysis and a second one also uses of the timing information). All three spectra agree well, as shown in the figure (main paper) as grey area, the envelope shape for 1σ errors of the spectra. The predicted energy resolution is ≈23%, reasonably constant above 150 GeV. Systematic errors of our detector (from atmospheric density and transmission uncertainties, the photon detection efficiency, non-linearity in the signal chain, limits in Monte Carlo simulations, choices in analysis cuts, etc.) are discussed in detail in (*15*). Uncertainties result in a possible systematic energy shift of up to ±20%, which translates into a shift of ∓25% in the limit set for the gamma ray horizon (energy for which the optical depth $\tau = 1$). The uncertainty in the spectral slope coefficient is ±0.2.

Attenuation of gamma rays from distant sources and EBL models

Absorption of high-energy gammas by the extragalactic background light (EBL) depends on the column density of low-energy photons traversed by the gamma rays. For gamma rays of observed energy E_γ, the maximal cross section for pair production at redshift z occurs at wavelength $\lambda = 1.24\,\mu\mathrm{m}(E_\gamma/1\,\mathrm{TeV})(1+\mathrm{z})^2$. Folded with the shape of the cross section, MAGIC's energy range specifically probes (with 3C 279) background wavelengths of 0.2 μm – 2 μm. This highlights the importance of the ultraviolet-to-near-infrared wavelength range in modifying the spectra of sources at gigaparsec distances (*16*). Knowledge of the amount of EBL along the line of sight to gamma ray sources is based on bolometric measurements and galaxy counts. Bolometric measurements are generally hampered by foreground emission in our own Galaxy (*17*). Since the light emitted from galaxies changes with time following the star formation history (*18*) and with the ageing stellar populations, the EBL has changed over time, too. An in-depth review can be found in (*19*).

Various models for the EBL have been published. In (*20*), several parameterized models using different assumptions for the evolving EBL are introduced, taking into account magnetic fields, gas and dust, the relative abundance of elements heavier than Helium, and the star formation rate. A range of parameters is proposed such that the results agree with what is known from deep galaxy surveys and infrared background measurements available in 2002. In a recent publication (*21*), two different backward-evolution EBL models were used to calculate the intergalactic photon density from $z = 0$ to $z = 6$ (called "Base" and 'Fast" evolution). In this report we use the "Fast" evolution model as predicting maximally *high* absorption. In a different publication (*22*), a semi-analytical forward-evolution approach was used to obtain the evolving EBL density. This model predicts a rather *low* EBL level at $z = 0$, just on top of the galaxy counts obtained from the Hubble Space Telescope (*18*). In fact, the model (*22*) predicts the EBL level at wavelengths above 5 μm slightly below the galaxy counts obtained from the Spitzer (*23, 24, 25*) data and the ISOCAM results (*26, 27*). The model (*22*) also lies below the FIRAS measurements in the far-infrared, an undershoot attributed to the abundance of Ultra-Luminous Infrared Red Galaxies (ULIRG), only recently discovered and not taken into account in the model. However, the EBL domain above 3 μm does not influence our result, given that the highest energy measured by MAGIC in the 3C 279 spectrum is below 500 GeV; EBL photons with $\lambda > 2.5$ μm do not reach the energy necessary for pair production. We have, therefore, chosen the model (*22*) as the *low* limit for the EBL level in the frequency range relevant for the MAGIC 3C 279 measurement.

In the discussion of the gamma ray horizon in the main paper, we have used a model tuned to give for 3C 279 the intrinsic photon index $\alpha^* = 1.5$. We call this ad-hoc EBL model maxEBL and give more details in the following. It is based on (*20*), with modified parameters. The "best-fit" model, defined in (*28*), is changed by reducing the optical and infrared star formation rate, by adding a "warm dust" component and by taking into account a high fraction of UV emission, which fits the data derived from AGN absorption lines, a method called proximity effect [e.g., (*29*)]. Additionally, the dust parameter for the optical galaxy component is set to a very low value of E(B-V) = 0.01, to account for the maximum possible optical flux. In detail, the parameters used [definition in (*20*)] are the following:
$\mathrm{SFR_{OPT}} : \alpha = 3.5, \beta = -1.2, z_p = 1.2, \dot{\rho_*}(z_p) = 0.08$,
$\mathrm{SFR_{LIG}} : \alpha = 4.5, \beta = 0.0, z_p = 1.0, \dot{\rho_*}(z_p) = 0.09$,
and further $f_{\mathrm{esc}} = 4, c_2 = 10^{-23.4}, E(B-V)_{\mathrm{OPT}} = 0.01$. Contrary to the "best-fit" EBL, the maxEBL model is above the emissivity data at wavelengths between 0.16 – 1.0 μm [(*20*) and references therein].

All EBL models mentioned contain the evolution of the radiation contributing to the EBL at different redshifts, and use the Lambda-CDM Universe with $\Omega_\lambda = 0.7$ and $\Omega_\mathrm{m} = 0.3$, confirmed by the latest results from the Wilkinson Microwave Anisotropy Probe (WMAP) (*30*). The models are graphically summarized in Fig. S2, along with a number of measurements.

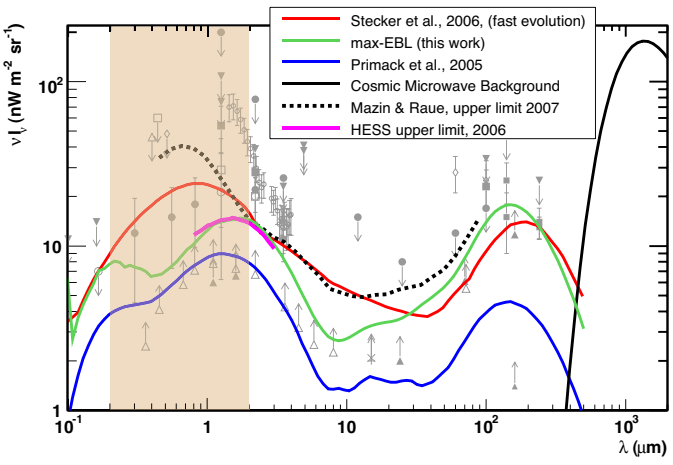

Fig. S2. EBL Models. Some of the models for EBL, for z=0, and measurements at various wavelengths. The green line is based on (*20*), with parameters adapted to the results from the latest galaxy counts. The dotted line is from (*31*). The shaded vertical band indicates the range of frequencies corresponding to the MAGIC observations.

Comparing the effect of different EBL models on our measured spectrum we add the following comments:

- The *high* model (*21*) leads to an intrinsic spectrum of 3C 279 with a (fitted) index of $\alpha^* = 0.5 \pm 1.2$ (see main paper), a rise in the VHE gamma ray spectrum very difficult to reconcile with extrapolation from EGRET data and with general constraints in the spectral energy distribution.

- The maxEBL model has been derived to be in agreement with an intrinsic blazar spectral index of $\alpha^* = 1.5$, and can be considered as an upper limit on the EBL density respecting the constraints from the measured VHE blazar spectra (*16, 31*). Note that the values for the optical and infrared star formation rate (SFR) and for the optical dust parameter are close to their lower limits, and no AGN contribution has been taken into account.

- The *low* EBL derived from (*22*) apparently gives an acceptable result, resulting in a most probable intrinsic power law with a spectral index $\alpha^* = 2.9 \pm 0.9$ (see main paper).

Some of the models discussed above seem less likely in the light of the present measurements, requiring the sources to exhibit a redshift-dependent hardening of their spectra. We should also note that the EBL density may be higher than derived here, if VHE photons are speculated to undergo interactions beyond standard physics [e.g., (*32*)].

Spectral Energy Distribution

Blazars represent the most violent variant of the AGN phenomenon, related to the activity of supermassive ($M = 10^8$–10^9 solar masses) black holes harbored in the center of galaxies. Their emission, extending from radio wavelengths to high-energy gamma rays, is produced within a jet of plasma ejected at relativistic speeds and pointing close to the Earth.

The spectral energy distribution (SED) of blazars is characterized by two broad bumps, the first one peaking between the infrared and the X-ray band, the second one in the gamma ray domain. The first peak traces the synchrotron emission of relativistic electrons spiraling along the lines of the magnetic field in the jets; the high-energy peak is presumably due to the inverse Compton scattering between these relativistic electrons and low-energy photons. The latter can be the synchrotron photons themselves [Synchrotron-Self-Compton (SSC) mechanism (*33*)] or ambient radiation [External-Compton (EC) mechanism (*34, 35*)]. Ambient radiation can enter the jet either from an accretion disk or from surrounding gas clouds. These models ultimately rely on electrons (or pairs) accelerated within the flow and thus are called *leptonic models*.

Other possibilities (*hadronic models*) involve gamma ray emission due to accelerated protons and ions. Such emission can result from pion production in hadronic interactions, pair production, or be due to synchrotron radiation [e.g., (*36, 37, 38, 39*)], and includes the associated production of neutrinos and ultrahigh-energy cosmic rays (*40*). Although the energy losses of protons and ions are suppressed by their large mass and the low matter density in the acceleration zone, they become sizeable at ultrahigh energies where photo-production of pions can take place in collisions with low-energy synchrotron photons.

Until now the majority of known extragalactic sources of VHE photons belongs to the class of BL-Lac objects, whose spectra show a weak signature of thermal radiation from outside the jet and hence favor the SSC scenario. In quasars [mostly Flat Spectrum Radio Quasars (FSRQs)], such as 3C 279 the situation with thermal radiation is different (the *blue bump* in the spectrum), and the EC process is likely to dominate if the gamma ray emission zone is close to the origin of the jet. The validity of the EC mechanism is not undisputed, however, since the gamma ray emission zone could well be far away from the central source of thermal radiation [e.g., (*41, 42*)].

Hadronic emission models require much larger magnetic field strengths than leptonic models, in order to confine the more massive and energetic particles to the jet. They generically produce harder VHE spectra than leptonic models. In low-peaked blazars at high redshifts such as FSRQs, however, the spectrum is steepened due to attenuation by the EBL, rendering differences in the spectra difficult to detect. 3C 279 is among the nearest FSRQs, and the energy threshold of MAGIC is low enough to permit observing this source.

The EGRET gamma ray telescope (operating in the past decade and sensitive between 20 MeV and few GeV) observed at several occasions bright and hard (photon index around 2) emission from 3C 279. In particular, during an extensive campaign held in 1996 the source showed a large (a factor 10 in amplitude) and short ($\sim$ 2-3 days) gamma ray flare (*4*) with episodes of relatively fast variability, including an increase by a factor of 2.6 in $\sim$8 hours. Naively extrapolating this behavior to the MAGIC band one could expect bright and short episodes also in this band. However, in the standard leptonic framework the detection of photons with energy above 100 GeV emitted by 3C 279 is somewhat surprising. Indeed, a careful consideration of the conditions expected in the source raises several problems, related to the high energy required for the electrons to emit photons with such high energy and the strong opacity to gamma rays expected inside these sources. The detection of strong VHE emission from 3C 279 thus is stretching leptonic models to or beyond their limits.

Emission model

The simplest EC model ("one-zone") assumes that the bulk of the emission is produced within a single region. In order to properly model the emission, good coverage of the entire SED is required, since only with known position and luminosity of both peaks is it possible to fully constrain the physical parameters [e.g., (*43*)]. In the case of the 3C 279 flare, we only have the simultaneous measurement in the optical R–band with the VHE spectrum derived by MAGIC. With this input we tried to reproduce the observed VHE spectrum assuming a simple one-zone model [see (*44*) for a full description].

The MAGIC observations contribute data to the important energy range above 10^{25}Hz, poorly studied thus far because lying above the range of satellite-borne instruments and below that of most ground-based Cherenkov telescopes. The SED in

Fig. S3 shows the MAGIC points corrected according to the two extreme EBL models discussed in the paper, together with measurements at lower frequencies from different epochs. In the same figure we show the generic one-zone model described here. The model uses the following assumptions and parameters: The source is spherical with radius $R = 5 \times 10^{16}$ cm, and it is in motion with a bulk Lorentz factor $\Gamma = 20$ at an angle $\theta = \Gamma^{-1} = 2.9$ deg with respect to the line of sight. The magnetic field has an assumed intensity $B = 0.15$ G. The particles, with a total density $n = 2 \times 10^4$ cm^{-3}, follow an energy distribution represented by a broken power law extending from $\gamma_1 = 1$ to $\gamma_2 = 3 \times 10^5$, with indices $n_1 = 2$ and $n_2 = 3.7$ below and above the break at $\gamma_p = 2.5 \times 10^3$. We model the external radiation field assuming that a fraction $\tau = 0.005$ of the disk emission, a black body with luminosity 6×10^{45} erg/s, is diluted into the Broad Line Region, a sphere with radius 4×10^{17} cm.

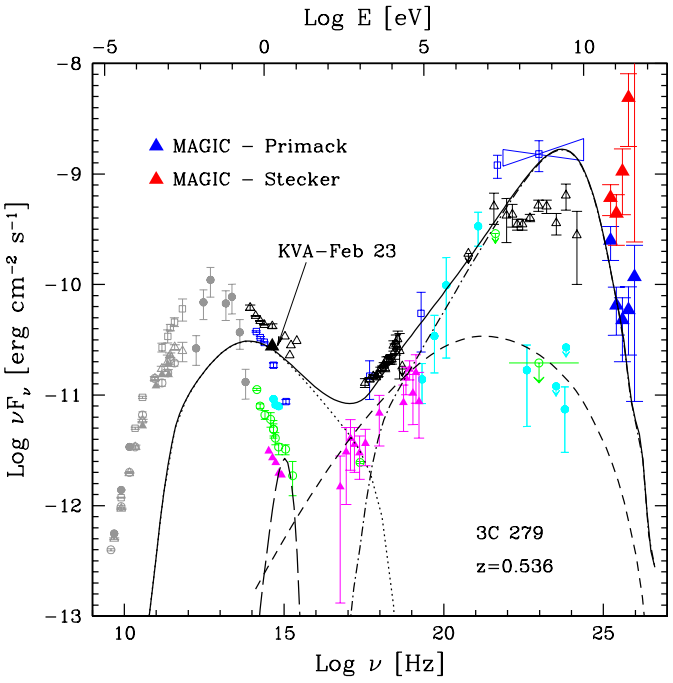

Fig. S3. Spectral energy distribution for 3C 279. Observations at different source intensities, over the years from 1991 to 2003, from (*45*) and (*46*), with MAGIC points (2006) at the high-energy end (right). The MAGIC points are corrected according to the two extreme EBL models of (*22*) and (*21*) (blue and red triangles, respectively); the former clearly gives a more probable result with a spectral index of $\alpha^* = 2.9 \pm 0.9$. An emission model and its individual components are also shown: the solid line represents the total model emission, fitted only to the (blue) MAGIC points and the (black) triangle from the KVA telescope. The individual components of the emission model are synchrotron radiation (dotted line), disk emission (long-dashed), synchrotron-self-Compton (short-dashed), and external Compton (dot-dashed).

Inverse-Compton peak

Accounting for attenuation of the gamma rays due to pair production in collisions with photons from the integrated light of galaxies, brings the emitted spectrum into agreement with models assuming inverse-Compton scattering of external photons as the dominant radiation process. The emitted spectrum also appears to be very similar to the spectra of many high-peaked BL-Lac objects, although their corresponding synchrotron peak is at much higher energies. In the framework of inverse-Compton scattering models this implies that external photon fields may act as scattering target, although seemingly not to the extent to create internal opacity due to pair production in photon-photon collisions (*47*). The inverse-Compton models predict a steep decline for two reasons: for one, the spectrum of the highest energy electrons, judging from the synchrotron spectrum, tends to be steep; and second, VHE electrons scatter with ambient photons in the Klein-Nishina regime, reducing the scattering efficiency. An EBL larger than the integrated light of known galaxies would imply that the generic leptonic emission models must undergo a major revision, perhaps involving proton synchrotron and cascade emission. The latter would shed new light on the correlation between active galactic nuclei and the directions of the highest energy cosmic rays (*48*).

References

1. A. Cavaliere, V. D'Elia, *Astrophys. J.* **571**, 226 (2002).
2. R. C. Hartman *et al.*, *Astrophys. J.* **385**, L1 (1992).
3. L. Maraschi *et al.*, *Astrophys. J.* **435**, L91 (1994).
4. A. E. Wehrle *et al.*, *Astrophys. J.* **497**, 178 (1998).
5. U. Bach *et al.*, *Astron. Astrophys.* **464**, 175 (2007).
6. W. Collmar *et al.*, *Multifrequency observations of the blazar 3C 279 in January 2006*, to be published in Proc. of the 6th INTEGRAL workshop "The Obscured Universe" (Moscow, July 2-8, 2006), eds. S. Grebenev, R. Sunyaev, C. Winkler, ESA SP 622 (2006) (preprint arXiv:0710.1096).
7. R. C. Hartman *et al.*, *Astrophys. J.* **553**, 683 (2001).
8. M. Boettcher *et al.*, *Astrophys. J.* **670**, 968 (2007).
9. M. Gaug *et al.* (MAGIC Collab.), *Calibration of the MAGIC Telescope*, Proc. of the 29th ICRC, Pune, 5-375, astro-ph/0508274 (2005).
10. T. Bretz *et al.* (MAGIC Collab.), *Standard Analysis for the MAGIC Telescope*, Proc. of the 29th ICRC, Pune, 5-315, astro-ph/0508274 (2005).
11. A. M. Hillas, in Proc. 19th International Cosmic Ray Conference, La Jolla (1985).
12. J. Albert *et al.*, *Nucl. Inst. Meth. A* **588**, 424 (2008).
13. T. Li, Y. Ma, *ApJ* **272**,317 (1983).
14. J. Albert et al., *Nucl. Inst. Meth. A* **583**, 494 (2007).
15. J. Albert *et al.*, *Astrophys. J.* **674**, 1037 (2007).
16. F. Aharonian *et al.*, *Nature* **440**, 1018 (2006).
17. K. Mattila, *Mon. Not. R. Astron. Soc.* **372**, 1253 (2006).
18. P. Madau, L. Pozzetti, *Mon. Not. R. Astron. Soc.* **312** L9 (2000).
19. M. G. Hauser, E. Dwek, *Ann. Rev. Astron. Astrophys.* **39**, 307 (2001).

20. T. M. Kneiske, K. Mannheim, D. H. Hartmann, *Astron. Astrophys.* **386**, 1 (2002).
21. F. W. Stecker, M. A. Malkan, S. T. Scully, *Astrophys. J.* **648**, 774 (2006).
22. J. R. Primack, J. S. Bullock, R. S. Somerville, *Observational Gamma Ray Cosmology*, In: High Energy Gamma Ray Astronomy, volume 745 of American Institute of Physics Conference Series, Eds. Aharonian, Voelk, and Horns, page 23 (2005).
23. G. Fazio *et al.*, *Astrophys. J. Suppl. Ser.* **154**, 39 (2004).
24. C. Papovich *et al. Astron. Astrophys. J. Suppl. Ser.* **154**, 70 (2004).
25. H. Dole *et al.*, *Astron. Astrophys.* **451**,417 (2006).
26. T. S. Metcalfe *et al.*, *Astron. Astrophys.* **407**, 791 (2003).
27. D. Elbaz *et al.*, *Astron. Astrophys.* **381**, 848 (2002).
28. T. M. Kneiske, T. Bretz, K. Mannheim, D. H. Hartmann, *Astron. Astrophys.* **413**, 807 (2004).
29. J. Scott *et al.*, *Astrophys. J. Suppl.* **130**, 67 (2000).
30. D. N. Spergel et al., *Astrophys. J. Suppl. Ser.* **148**, 175 (2003).
31. D. Mazin, M. Raue, *Astron. Astrophys.* **471**, 439 (2007).
32. A. De Angelis, M. Roncadelli, O. Mansutti, *Phys. Rev. D* **76**, 121301 (2007)
33. L. Maraschi, G. Ghisellini, A. Celotti, *Astrophys. J.* **397**, L5 (1992).
34. C. D. Dermer, R. Schlickeiser, *Astrophys. J.* **416**, 458 (1993).
35. M. Sikora, M. C. Begelman, M. J. Rees, *Astrophys. J.* **421**, 153 (1994).
36. K. Mannheim, *Astron. Astrophys.* **269**, 67 (1993).
37. K. Mannheim, P. L. Biermann, *Astron. Astrophys.* **251**,L 21 (1992).
38. F. A. Aharonian, *New Astronomy* **5**, 377 (2000).
39. A. Mücke, R. J. Protheroe, R. Engel, J. P. Rachen, T. Stanev, *Astroparticle Physics* **18**, 593 (2003).
40. K. Mannheim, T. Stanev, P. L. Biermann, *Astron. Astrophys.* **260**, L1 (1992).
41. E. J. Lindfors, E. Valtaoja, M. Türler, *Astron. Astrophys.* **440**, 845 (2005).
42. E. J. Lindfors *et al.*, *Astron. Astrophys.* **456**, 895 (2006).
43. F. Tavecchio, L. Maraschi, G. Ghisellini, *Astrophys. J.* **509**, 608 (1998).
44. L. Maraschi, F. Tavecchio, *Astrophys. J.* **593**, 667 (2003).
45. L. Ballo *et al.*, Spectral Energy Distributions of 3C 279 Revisited, *Astrophys. J.* **567**, 50 and references therein (2002).
46. W. Collmar *et al.*, Proceedings of the 5th INTEGRAL Workshop on the INTEGRAL Universe (ESA SP-552), 16-20 February 2004, Munich, Germany. p.555, (2004).
47. A. Reimer, *Astrophys. J.* **665**, 1023 (2007).
48. J. Abraham *et al.* (The Pierre Auger Collaboration), *Science* **318**, 938 (2007).